The Basic Attractor of the Viscous Moore-Greitzer Equation

Björn Birnir [*,†] and Höskuldur Ari Hauksson [*,‡]

October 22, 1999

Abstract

The basic attractor of nonlinear partial differential equations is the part of the global attractor that attracts a prevalent set in phase space. We give a qualitative description of stall, which is a component of the basic attractor. The basic attractor can contain more than one stall component. The existence of these components is proven and their stability explored. Numerical results are presented, showing the shape and evolution of stall cells over large parameter regions.

1 Introduction

In recent years a lot of attention has been devoted to the study of air flow through turbomachines. Under certain operation parameter values the air flow through modern jet engines is unstable. In order to avoid these instabilities the engines are designed so that their optimal operation parameter values are far from the instability boundaries. This leads to an engine design that is unnecessarily heavy and fuel inefficient.

A jet engine can be thought of as a compressor, where the incoming air is compressed by alternating rings of rotating blades, or rotors, and stationary blades, or stators. The mixture of fuel and compressed air is then ignited and the resulting combustion generates thrust that propels the aircraft. Numerical and experimental evidence indicates that there are three types of instabilities that occur in the flow through the compressor. They are called *stall*, *surge* and *classic surge*. Surge is characterized by large oscillations of the mean mass flow through the engine. During part of the cycle, the mean mass flow may become reversed, thrusting air out the front of the engine. This puts a large stress on the components of the engine and seriously impairs its performance. When stall occurs, there are regions of relatively low air flow that form at isolated locations around the rim of the compressor. Here too, the phenomenon can be so pronounced that the flow in these isolated regions is reversed. Again this causes a large stress on the components of the engine and reduces its performance. Classic surge appears to be a more complicated motion which can probably be best described as a mixture of surge and stall.

Our goal is to understand these instabilities better in the framework of the viscous Moore-Greitzer partial differential equation and ultimately to design control strategies for recovering design

[*]Department of Mathematics, University of California Santa Barbara, Santa Barbara, CA 93106 and Science Institute, University of Iceland, 3 Dunhaga, IS-107 Reykjavik, Iceland

[†]birnir@math.ucsb.edu

[‡]hauksson@math.ucsb.edu

flow after the system has been thrown into stall, surge or classic surge. If successful, such a control strategy could lead to jet engine design which is lighter and more fuel efficient. To facilitate this, a better understanding of the behaviour of the air flow during stall, surge and classic surge is necessary. In our paper [6] we proved the well posedness and the existence of a finite dimensional attractor for the viscous Moore-Greitzer turbomachine model. In the present paper we analyze stall, wich is a part of the core of this attractor, the basic attractor. We show that there can exist a small number of stall solutions and we analyze their stability.

Moore and Greitzer published in 1986 a PDE model for turbomachines which has been very successful [22]. A substantial amount of work has been done on finite Galerkin approximations of that model since, see e.g. [19] [17] and references therein. Banaszuk *et al.* [2] considered the full PDE model of Moore and Greitzer.

The Moore-Greitzer model is a continuum actuator disk model for flow through discrete blade passages in the compressor. The question then becomes how a finite Galerkin truncation of this PDE/ODE model can capture anything about a compressor with a finite number of rotor and stator blades. In this paper we will make precise what qualitative information may be captured by such a truncation, but we will also provide the nonlinear stall modes that permit one to capture quantitative information as well.

Currently Mezić [20] has derived a model of the three dimensional flow in jet engine compressors. His model reduces to that presented in [6] when one assumes that the dependence of the flow on the radial direction is negligable. The viscous term in that equation, first introduced by Adomaitis and Abed [1], has however a new and better interpretation in Mezić's treatment. The term is not due to the viscosity of the air, but rather, it is a diffusion term due to the inviscid process of turbulent momentum transport via Reynolds stresses. The difference is several orders of magnitude of the constant ν, which now represents the eddy viscosity.

In our article [6] we proved that the Moore-Greitzer PDE model with viscosity has a unique solution in the Hilbert space $X = \bar{H}^1 \times \mathbf{R}^2$ where $\bar{H}^1$ denotes the Sobolev space with index one of functions on the unit circle with square integrable first derivative and zero mean. We also proved that this solution is smooth in space and time variables. Finally we proved that this dynamical system has a global attractor with finite Hausdorff and fractal dimensions and we presented explicit estimates for the dimensions.

Experimental, numerical and analytical results indicate that the stable solutions of the global attractor can be classified into the following groups: axisymmetric design flow, surge, classic surge and stall. Surge has been fully analyzed [22] [19]. Stall has only been analyzed in finite Galerkin approximations [22] [19] [17], but classic surge is the least understood of these groups [18]. Our goal here is to give a complete description of stall for a large parameter range.

The requirement that every point (function) of an attractor attracts a set of positive "infinite-dimensional" measure seems to be much more restrictive than just to require a point to be attracting. Accordingly the basic attractors that are known are low-dimensional whereas attractors can in general be very high-dimensional. The basic attractor found here is the first complex one, to our knowledge, to be explicitly known for a parabolic PDE/ODE system. It is surprising that it can have such a rich structure for a parabolic system which typically are gradient systems with attractors consisting of sinks and saddles. We do not try to present here a bifurcation theory of the basic attractors, nor prove analytically that the description of the basic attractor is complete (global) for the parameter regions in question. However, this has been checked numerically and the tools developed in this paper can be used to explore the bifurcations of basic attractors including the development of classic surge. This is however a topic for an other publication. Perhaps most importantly for a dynamical systems theory of PDEs, some of the results in this paper point to a notion of control for infinite-dimensional systems, this will be explored in still another publication.

In the following two subsections we will first introduce the equations of motion and the assumptions made in their analysis. Then the concept of a basic attractor [21] is well known in the setting of finite dimensional dynamical systems, but less so in the infinite dimensional setting. For completeness we give a brief introduction to it here. In section 2 we derive explicit stall solutions and their stability is analyzed in section 3. In section 4 we analyze for what parameter range our results are valid. We then present the results of numerical simulations in section 5 which exhibit surge and stall solutions and compare these stall solutions with the explicit ones. Furthermore, we present numerical results on the stability of stall.

1.1 The Equations of Motion

We will from now on focus our attention on Mezić's model [20], but with the additional assumption that the flow is independent of the radial coordinate. For compressors with straight exit ducts, the equations of motion become the same as those analyzed in [6]. Following Banaszuk *et al.* [2] one can introduce the operator K which acts in Fourier spaces as follows

$$K\left(\Phi + \sum_{n\in\mathbf{Z}\setminus\{0\}} \varphi_n e^{in\theta}\right) = \Phi + \sum_{n\in\mathbf{Z}\setminus\{0\}} \left(1+\frac{am}{|n|}\right)\varphi_n e^{in\theta}$$

and then the equations of motion can be written as

$$\frac{\partial}{\partial t}\varphi = K^{-1}\left(\nu\frac{\partial^2\varphi}{\partial\theta^2} - \frac{1}{2}\frac{\partial\varphi}{\partial\theta} + \psi_c(\Phi+\varphi) - \overline{\psi_c}\right), \quad \theta\in[0,2\pi] \tag{1}$$

$$\frac{d\Phi}{dt} = \frac{1}{l_c}(\overline{\psi_c} - \Psi) \tag{2}$$

$$\frac{d\Psi}{dt} = \frac{1}{4l_cB^2}(\Phi - \gamma F_T^{-1}(\Psi)) \tag{3}$$

where

$$\overline{\psi_c} := \frac{1}{2\pi}\int_0^{2\pi} \psi_c(\Phi(t)+\varphi(t,\theta))d\theta.$$

The variable θ represents the circumferential coordinate of the compressor, t is time. Φ and Ψ are respectively the mean flow and pressure rise over the compressor. φ is the disturbance from the mean flow Φ, and the two functions $\overline{\psi_c}$ and $F_T^{-1}(\Psi)$ describe the pressure change over the compressor and throttle respectively.

We will make the following assumptions: The operator K is the identity. This is true for jet engines that have many stages of rotating and stationary blades. The case when K is not the identity applies to compressors that have ideal inlet guide vains and few stages of rotating and stationary blades [20]. In fact, K can be written as a sum of the identity and a compact operator, $K = I + R$, and the norm of R is $\|R\| = am$. We prove in section 4 that our analysis is also valid when K is close to being the identity. The constant am is inversely proportional to rotor velocity and the number of stages in the compressor. The compressor characteristic ψ_c is a cubic polynomial with a negative leading coefficient and F_T^{-1} is a smooth function which is identical to $F_T^{-1}(\Psi) = \Psi|\Psi|^{-1/2}$ outside a small neighbourhood of the origin.

1.2 Basic Attractors

The notion of a basic attractor was first introduced by Milnor [21] in the setting of finite dimensional dynamical systems. This idea was later extended to infinite dimensional dynamical systems by Birnir and Grauer [3]. For completeness sake we include here a brief introduction to this theory. We consider a dynamical system in a Banach space X whose trajectories are given by $x(t) = S(t)x_o$ where $S(t)$ is the evolution operator and x_o denotes the initial state.

We say that a set M is *invariant* under the flow if $S(t)M = M$, i.e. M is both positively and negatively invariant. An *attractor* $\mathcal{A}$ is an invariant set which attracts a neighborhood U or for all $x_o \in U$, $S(t)x_o$ converges to $\mathcal{A}$ as $t \to \infty$. The largest such set U is called the *basin of attraction* of the attractor $\mathcal{A}$. If the basin of attraction of an attractor $\mathcal{A}$ contains all bounded sets of X and $\mathcal{A}$ is compact, then we say that $\mathcal{A}$ is the *global attractor*.

It has been shown (see Birnir and Hauksson [6]) that the equations of motion (1-3) have a global attractor which is smooth and has finite Hausdorff and fractal dimensions. The dimension estimates are however fairly large and not necessarily a good indication of the size of the attractor.

In this paper we focus on the core of the attractor $\mathcal{A}$ which is called the basic attractor $\mathcal{B}$. For now, let us assume that the Banach space X is finite dimensional. An attractor $\mathcal{B}$ is called a *basic attractor* if,

- The basin of attraction of $\mathcal{B}$ has positive measure.
- There exists no strictly smaller $\mathcal{B}' \subset \mathcal{B}$, such that up to sets of measure zero, $basin(\mathcal{B}) \subset basin(\mathcal{B}')$.

A *global basic attractor* is a basic attractor whose basin of attraction contains all bounded sets of X up to sets of measure zero.

From now on we will assume that all attractors are global and we will omit the word global when refering to them. This will not cause confusion.

A theorem by Milnor [21] states that in finite dimensions there exists a unique decomposition of the attractor $\mathcal{A}$,

$$\mathcal{A} = \mathcal{B} \cup \mathcal{C}$$

where $\mathcal{B}$ is a basic attractor and $\mathcal{C}$ is a remainder such that $m(basin(\mathcal{C}) \backslash basin(\mathcal{B})) = 0$ where m is the Lebesque measure.

The notion of a basic attractor can be extended to infinite dimensions and Milnor's Theorem was first proven in an infinite-dimensional setting by Birnir and Grauer [3]. It requires an extension of the concepts of measure zero and almost every. Their counterparts in infinite dimensions are *shy* and *prevalent* sets respectively (see Hunt *et al.* [11]). These are defined in the following way. Let X denote a Banach space. We denote by $S + v$ the translate of the set $S \subset X$ by a vector v. A measure μ is said to be *transverse* to a Borel set $S \subset X$ if the following two conditions hold:

- There exists a compact set $U \subset X$ for which $0 < \mu(U) < \infty$.
- $\mu(S + v) = 0$ for every $v \in X$.

A Borel set $S \subset X$ is called *shy* if there exists a compactly supported measure transverse to S. More generally, a subset of X is called shy if it is contained in a shy Borel set. The complement of a shy set is said to be a *prevalent* set.

The infinite-dimensional analog of Milnor's Theorem can now be stated,

Theorem 1.1 *Let $\mathcal{A}$ be the compact attractor of a continuous map $S(t)$ on a separable Banach space X. Then $\mathcal{A}$ can be decomposed into a maximal basic attractor $\mathcal{B}$ and a remainder $\mathcal{C}$,*

$$\mathcal{A} = \mathcal{B} \cup \mathcal{C}$$

such that the realm of attraction of $\mathcal{B}$ is prevalent but the realm of attraction of $\mathcal{C}$, excluding points that are attracted to $\mathcal{B}$, is shy.

For a proof of this Theorem see Birnir [5]. The realm of attraction is a slight generalization of the basin of attraction, as the basin is an open set, but the realm can be either open or closed.

For systems that are simple enough, the basic attractor contains only the stable trajectories of the global attractor. When transients are ignored, one will only see the basic attractor in physical and numerical experiments and not the remainder $\mathcal{C} = \mathcal{A} \backslash \mathcal{B}$ of the attractor. All the relevant dynamics are therefore contained in the basic attractor.

2 Explicit Solutions for Stall

Experimental and numerical evidence indicate that the basic attractor in axial compression systems is low dimensional [7] [8] [9] [24]. It consists of axisymmetric design flow, surge, classic surge and stall. The design flow is a stationary solution and surge is a periodic cycle which has been well studied (see [22] and [19]). It only involves the two ODEs in the system (1-3). Stall has been studied in low order Galerkin truncations of the Moore-Greitzer equations [19] [17].

The goal of this paper is to analyze stall in the viscous Moore-Greitzer equation, justified by Mezić [20], with the additional assumptions introduced above. Experimental and numerical evidence indicate that the two ODE variables Φ and Ψ are independent of time in stall and that we have a traveling wave solution

$$\varphi(t, \theta) = \varphi(\eta), \quad \eta = \theta - \alpha t$$

where α is the constant propagation speed of the wave around the annulus. We will therefore look for solutions of this form. We refer to the (t, η)-plane as the rotating reference frame and the (t, θ)-plane as the fixed reference frame.

Observe that when φ is a traveling wave that has a fixed profile and the mean flow Φ is constant, then the angular averaged pressure rise $\overline{\psi_c}$ is constant. With the above assumptions the system (1-3) reduces to a single ODE with periodic boundary conditions coupled to two algebraic equations

$$\begin{aligned} 0 &= \nu\varphi'' + (\alpha - \tfrac{1}{2})\varphi' + \psi_c(\Phi + \varphi) - \overline{\psi_c} \\ 0 &= \begin{bmatrix} \frac{1}{l_c}(\overline{\psi_c} - \Psi) \\ \\ \frac{1}{4 l_c B^2}\Phi - \gamma F_T^{-1}(\Psi)) \end{bmatrix} = G_\gamma(\Phi, \Psi, \varphi). \end{aligned} \tag{4}$$

Here the prime denotes differentiation with respect to η.

In general the ODE and the algebraic equations will have to be solved simultaneously, but as we shall see in Lemma 2.1, there exists a special solution of the algebraic equations which places only small restrictions on the solution φ. We can therefore seek a solution of the ODE in a large class without regard for the algebraic equations.

Lemma 2.1 *There exist γ_*, Φ_*, Ψ_* such that*

1. *For $\Phi = \Phi_*$ we have*
$$\psi_c(\Phi + \varphi) - \psi_c(\Phi) = -b\varphi^3 + c\varphi$$
for some constants b, c.

2. *For all $\varphi \in \bar{H}^1$ such that $\int_0^{2\pi} \varphi^3(\theta)d\theta = 0$, we have*
$$G_{\gamma_*}(\Phi_*, \Psi_*, \varphi) = 0.$$

Proof: The compressor characteristic ψ_c is a cubic polynomial with a negative leading coefficient. If we define
$$h_\Phi(x) = \psi_c(\Phi + x) - \psi_c(\Phi)$$
then $h_\Phi(0) = 0$ and h_Φ is also a cubic polynomial with a negative leading coefficient. Let Φ_* be the unique number such that h_{Φ_*} is an odd function. Then
$$h_{\Phi_*}(x) = -bx^3 + cx$$
and the first part of the Lemma is complete.

Now set $\Psi_* = \psi_c(\Phi_*)$ and $\gamma_* = \frac{\Phi_*}{F_T^{-1}(\Psi_*)}$, then
$$G_{\gamma_*}(\Phi_*, \Psi_*, 0) = 0.$$
Let φ satisfy the assumptions in the Lemma. Recall that since $\varphi \in \bar{H}^1$, it has zero average. We have
$$\begin{aligned} \int_0^{2\pi} h_{\Phi_*}(\varphi(\theta))d\theta &= -b\int_0^{2\pi} \varphi^3(\theta)d\theta + c\int_0^{2\pi} \varphi(\theta)d\theta \\ &= 0 \end{aligned}$$
and thus
$$\overline{\psi_c} = \psi_c(\Phi_*) = \Psi_*.$$
We conclude that
$$G_{\gamma_*}(\Phi_*, \Psi_*, \varphi) = 0$$
and the Lemma is proven. □

For now we shall assume that γ, Φ, Ψ have been chosen as the specific values given by Lemma 2.1. This assumption is rather restrictive, but in section 4 we show that it can be relaxed. With this choice, our problem is reduced to finding a solution of the equation
$$0 = \nu\varphi'' + (\alpha - \frac{1}{2})\varphi' - b\varphi^3 + c\varphi$$
on the unit circle, subject to the constraints $\int_0^{2\pi} \varphi^3(\theta)d\theta = 0$ and $\varphi \in \bar{H}^1$.

Applying Hamiltonian methods, we consider this equation as an evolution equation and look for periodic solution with the correct period to satisfy the periodic boundary conditions in the boundary value problem. The correct periods are $T = \frac{2\pi}{n}$ where n is a positive integer. This equation is the well known Duffing's equation. The constant $\alpha - \frac{1}{2}$ appears as damping which can be either positive, negative or zero. It is a known fact that for nonzero damping, the Duffing's equation has no periodic solutions. We must therefore restrict ourselves to the case when $\alpha = \frac{1}{2}$. The reader is refered to Guckenheimer and Holmes [13] and Lawden [15] for a further discussion of Duffing's equation.

Proposition 2.1 *For $\alpha = \frac{1}{2}$ there exist N solutions of equation (4) given by (Φ, Ψ, φ_j), $j = 1, ..., N$, where*

$$\varphi_j(\eta) = \sqrt{\mu_j} ns(\omega_j \eta + i\hat{\omega}_2, k_j)$$

and

$$\mu_j = 2\frac{c}{b}(1 + \sqrt{1 - (\frac{b}{c})^2 \bar{c}_j}), \quad \omega_j = \sqrt{\frac{b\mu_j}{2\nu}}, \quad k_j = \frac{1 - \sqrt{1 - (\frac{b}{c})^2 \bar{c}_j}}{1 + \sqrt{1 - (\frac{b}{c})^2 \bar{c}_j}}, \quad N \leq [\sqrt{\frac{c}{\nu}}]$$

where $[\cdot]$ denotes the integer part, $\bar{c}_j$ are constants of integration, ns is the Jacobi elliptic function, see [23], and $i\hat{\omega}_2$ is half the imaginary period of ns.

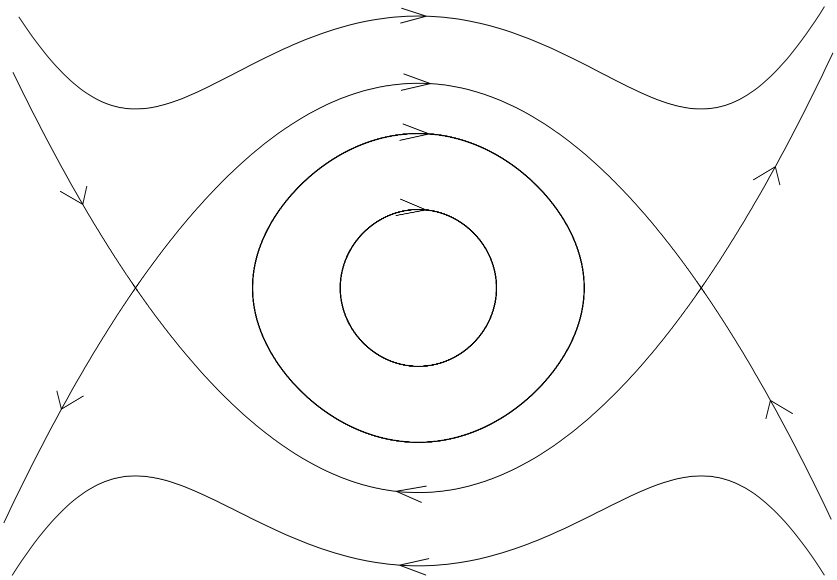

Figure 1: This figure shows the phase portrait for the Duffing's equation.

Proof: Writing the ODE in (4) as a first order system one gets

$$\begin{aligned} \dot{x} &= y \\ \dot{y} &= \tfrac{1}{\nu}(bx^3 - cx). \end{aligned}$$

The only periodic cycles lie inside the heteroclinic orbit, see Figure 1. The period of these cycles is bounded below by the period of the linearized system T_{lin}, linearized about the center.

The period then tends monotonically to infinity as we pick cycles closer to the heteroclinic orbit. The period of the system linearized about the origin (harmonic oscillator) is

$$T_{lin} = 2\pi\sqrt{\frac{\nu}{c}}.$$

We are looking for periodic orbits which have periods $T_j = \frac{2\pi}{j}$ and due to the lower bound on the periods offered by the linear system we can bound their number by

$$N \leq [\sqrt{\frac{c}{\nu}}]. \tag{5}$$

Multiplying through Duffing's equation with $\frac{d\varphi}{d\eta}$ and integrating once we obtain

$$\left(\frac{d\varphi}{d\eta}\right)^2 = \frac{b}{2\nu}(\varphi^4 - \frac{2c}{b}\varphi^2 + \bar{c})$$

where $\bar{c}$ is a constant of integration. One can use quadratures to integrate this equation. By recalling that the Jacobi elliptic function ns satisfies the differential equation

$$(ns')^2 = (ns^2 - 1)(ns^2 - k^2)$$

where k is the modulus, one quickly verifies that the solution is given by

$$\varphi(\eta) = \sqrt{\mu}ns(\omega\eta + i\hat{\omega}_2, k),$$

where the Jacobi elliptic function ns is shifted half way up its period parallelogram by $i\hat{\omega}_2$, compare [4], to make it real and non-singular. What remains is to pick out the correct orbits and that is done by choosing the correct constants of integration. Since ns is an odd function, it is trivial to verify that it satisfies the conditions in Lemma 2.1. □

The constants of integration can be determined by using an identity relating the period of ns to the modulus

$$T = 4\int_0^1 \frac{dt}{\sqrt{(1-t^2)(1-k^2t^2)}}.$$

In our case this becomes

$$T_j = \frac{2\pi}{j} = \frac{4}{\omega_j}\int_0^1 \frac{dt}{\sqrt{(1-t^2)(1-k_j^2t^2)}} \tag{6}$$

which can now be solved to give $\bar{c}_j$.

The constants of integration lie on the interval $\bar{c}_j \in [0, (\frac{c}{b})^2]$. Using this fact along with the above formula for the periods, T_j, one can obtain the exact number N of periodic orbits.

3 Stability of Stall Cell

We have now constructed special solutions which describe stall. The next step is to analyze their stability. As we shall see, once one has analyzed the stability for the first stall solution, one has in effect analyzed the stability of all of them. We will therefore focus our attention only on the first one (Φ, Ψ, φ_1) and drop the subscript 1.

The stall solutions given by Proposition 2.1 are periodic in both space and time. We will in the sequel prove that these solutions are asymptotically orbitally stable. When proving asymptotic orbital stability of periodic orbits, one typically considers the Poincaré map associated with the orbit. To be more specific, one proves that the spectrum of the linearized Poincaré map lies in a closed subset of the open unit disk. To find the spectrum of the linearized Poincaré map, we study the full linearized system, i.e. the system (1-3) linearized about a stall solution, in the rotating reference frame. The stall solutions are stationary solutions in the rotating reference frame. It turns out that the spectrum of the full linearized system is related to the spectrum of the Lamé potential, which was studied by Hermite [10] early this century. Due to this connection to the Lamé potential, we are able to find analytically the eigenvalues and eigenvectors of the full linearized system, which in turn gives us the eigenvalues and eigenvectors of the linearized Poincaré map.

We begin by studying equation (1) linearized in $\bar{H}^1$. When the average term, $\overline{\psi_c}$, is neglected, the linearized equation can be written as

$$\frac{\partial u}{\partial \xi} = \nu \frac{\partial^2 u}{\partial \eta^2} - 3b\varphi^2 u + cu, \tag{7}$$

where $\xi = t + 2\theta$ and the effect of the average term $\overline{\psi_c}$ will be calculated in Proposition 3.1. Before we substitute in the stall solution we found in last section, we can utilize a relationship between the Jacobi elliptic function ns and the Weierstrass $\wp$-function (see Du Val [23]), namely

$$ns^2 = \wp - e_2$$

where $e_1 \geq e_3 \geq e_2$ are the stationary values of $\wp$. (We are following the convention in [23] for the ordering of the stationary values.) The right hand side of equation (7) now becomes

$$\nu \frac{\partial^2}{\partial \eta^2} - 3b\mu(\wp(\omega\eta + i\hat{\omega}_2) - e_2) + c.$$

By making the substitution $s = \omega\eta$, we can rewrite this as

$$\frac{b\mu}{2}\left(\frac{\partial^2}{\partial s^2} - 6\wp(s + i\hat{\omega}_2) + 6e_2 + \frac{2c}{b\mu}\right). \tag{8}$$

This is a constant translate of the Lamé operator (see [16] and [4])

$$\frac{\partial^2}{\partial s^2} - 6\wp.$$

We have the following lemma,

Lemma 3.1 *The Lamé operator*

$$\frac{\partial^2}{\partial s^2} - 6\wp$$

in L^2 has five simple eigenvalues

$$(\lambda_1, \lambda_2, \lambda_3, \lambda_4, \lambda_5) = (\sqrt{3g_2}, -3e_2, -3e_3, -3e_1, -\sqrt{3g_2}),$$

where $g_2 = -4(e_1e_2 + e_2e_3 + e_3e_1)$, with corresponding eigenfunctions

$$\begin{aligned}
\phi_1 &= \wp(s) - \sqrt{\tfrac{g_2}{12}} \\
\phi_2 &= cs(s)ds(s) \\
\phi_3 &= ns(s)cs(s) \\
\phi_4 &= ns(s)ds(s) \\
\phi_5 &= \wp(s) + \sqrt{\tfrac{g_2}{12}}.
\end{aligned}$$

The rest of the spectrum consists of a decreasing sequence of negative double eigenvalues $\{\lambda_j\}_{j=6}^{\infty}$, which tend to negative infinity as j gets larger. The eigenfunctions form a complete basis for $L^2([0,T])$ where T is the real period of $\wp$.

The above applies equally well to H^1, where H^1 denotes the Sobolev space with index one of functions on the unit circle with square integrable derivatives. In particular, H^1 contains $\bar{H}^1$ as a subspace of codimension one.

Proof: See Magnus and Wrinkler [16], Ince [12] and Birnir [4]. $\square$

Using the fact that $e_1 + e_2 + e_3 = 0$ and $e_1 \geq e_3 \geq e_2$ one quickly verifies that $\lambda_j \geq \lambda_{j+1}$. We need to determine how much the spectrum of the Lamé potential is shifted by the constant $6e_2 + \frac{2c}{b\mu}$. It has already been shown that $\varphi = \sqrt{\mu}ns(\omega\eta + i\hat{\omega}_2, k)$ satisfies the equation

$$0 = \nu\frac{\partial^2}{\partial\eta^2}\varphi - b\varphi^3 + c\varphi.$$

Differentiating this equation once with respect to η, we get

$$0 = (\nu\frac{\partial^2}{\partial\eta^2} - 3b\varphi^2 + c)\varphi'$$

and thus, $\varphi' = Cns' = Ccsds$ is an eigenfunction of equation (7) with zero eigenvalue. This happens also to be an eigenfunction of the Lamé operator with eigenvalue $-3e_2$. This implies that the spectrum of the operator given by equation (8), is the spectrum of the Lamé potential shifted by $3e_2 < 0$, i.e. the spectrum is

$$(\tilde{\lambda}_1, \tilde{\lambda}_2, \tilde{\lambda}_3, \tilde{\lambda}_4, \tilde{\lambda}_5) = \frac{b\mu}{2}(\sqrt{3g_2} + 3e_2, 0, -3(e_3 - e_2), -3(e_1 - e_2), -\sqrt{3g_2} + 3e_2),$$

and

$$\mu = -\frac{2c}{3be_2}.$$

We conclude, that when we consider only equation (1) and ignore its average term and linearize it with respect to disturbances in H^1, we get one-dimensional unstable and one-dimensional center spaces and a stable eigenspace of codimension two.

We now need to consider the full system from section 1.1 linearized about the stall solution. Its right hand side is

$$E \begin{bmatrix} \varphi \\ \Phi \\ \Psi \end{bmatrix} = \begin{bmatrix} \nu \frac{\partial^2}{\partial \eta^2} + \psi_c' - \overline{\psi_c'} & \psi_c' - \overline{\psi_c'} & 0 \\ \frac{1}{l_c}\overline{\psi_c'} & \frac{1}{l_c}\overline{\psi_c'} & -\frac{1}{l_c} \\ 0 & \frac{1}{4l_c B^2} & -\frac{\gamma}{4 l_c B^2}(F_T^{-1})' \end{bmatrix} \begin{bmatrix} \varphi \\ \Phi \\ \Psi \end{bmatrix}, \tag{9}$$

where ψ_c' and $\overline{\psi_c'}$ denote the Fréchet derivatives of ψ_c and $\overline{\psi_c}$ respectively.

Proposition 3.1 *The stall solution (Φ, Ψ, φ) is an asymptotically orbitally stable periodic orbit if the real parts of the eigenvalues of the restriction of the operator E to the subspace span$\{(\wp - \overline{\wp}, 0, 0), (0,1,0), (0,0,1)\}$ have negative real parts. Here $\overline{\wp}$ denotes the average of $\wp$. If there exists an eigenvalue of the restricted operator with a positive real part then the stall solution is unstable.*

Remark 3.1 The significance of this proposition is that we only need to consider the eigenvalues of a 3×3 matrix in order to determine the stability of stall solutions.

It also tells us that if we want to use a low order Galerkin projection to approximate the flow close to the special solution (Φ, Ψ, φ), then one should include the vector $(\wp - \overline{\wp}, 0, 0)$ in the set of vectors that one projects onto.

Proof: If the spectrum of the linearized Poincaré map lies in a closed subset of the open unit disk, then the periodic orbit is asymptotically orbitally stable. If on the other hand there exists an eigenvalue outside the unit disk, then the orbit is unstable. Before we find the spectrum of the linearized Poincaré map associated with the stall solution, we need to determine the spectrum of the operator E given by equation (9).

Let $\phi \in H^1 \backslash \text{span}\{\phi_1, \phi_5\}$. Since eigenspaces corresponding to different eigenvalues are orthogonal and $\text{span}\{\phi_1, \phi_5\} = \text{span}\{\wp, \underline{1}\}$, we know that $\langle \phi, 1 \rangle = 0$ and thus $\phi \in \bar{H}^1$. Furthermore, since $\psi_c' \in \text{span}\{\phi_1, \phi_5\}$, we have $\overline{\psi_c'}\phi = \langle \psi_c', \phi \rangle = 0$. We can now conclude that if ϕ lies in an eigenspace of the translated Lamé potential corresponding to the eigenvalue λ, then $(\phi, 0, 0)$ lies in an eigenspace of E corresponding to the same eigenvalue. Let Q be the subspace spanned by all such functions and notice that we have $EQ \subset Q$.

For any $\phi \in H^1 \backslash \text{span}\{\phi_1, \phi_5\} \subset \bar{H}^1$, we have $(\phi, 0, 0) \in Q$ and we can conclude that codim(Q) in $H^1 \times \mathbf{R}^2$ is 4. Since $Q \subset \bar{H}^1 \times \mathbf{R}^2$, we can also conclude that codim(Q) in $\bar{H}^1 \times \mathbf{R}^2$ is 3. The orthogonal complement of Q is $Q^\perp = \text{span}\{(\wp - \overline{\wp}, 0, 0), (0,1,0), (0,0,1)\}$ and one quickly verifies that $EQ^\perp \subset Q^\perp$. From all of the above we conclude that the spectrum of E is

$$\sigma(E) = \sigma(E|_Q) \cup \sigma(E|_{Q^\perp}).$$

We know that Q contains a one dimensional center subspace corresponding to direction of propagation of the stall solution and the rest of Q belongs to the stable subspace of E. Furthermore, Q has a complete basis of eigenvectors. If λ_n is a non-zero eigenvalue of E with an eigenvector χ_n, then $\mathrm{e}^{\lambda_n t}\chi_n(\eta)$ is a solution of the full linearized system in the rotating reference frame. Then $\mathrm{e}^{\lambda_n t}\chi_n(\theta - \frac{1}{2}t)$ is a solution of the full linearized system in the fixed reference frame. If χ_n is a $2\pi/m_n$ periodic solution it will give us an eigenvalue of the linearized Poincaré map $\mu_n = \mathrm{e}^{4\pi\lambda_n/m_n}$ with the corresponding eigenvector χ_n.

If the 3×3 matrix $E_{Q^\perp}$ has three eigenvectors, then we have the complete spectrum of the linearized Poincaré map. In particular, if $E_{Q^\perp}$ has an eigenvalue with a positive real part, then the linearized Poincaré map will have an eigenvalue outside the unit disk and the periodic orbit is unstable. Let us now assume that all eigenvalues of $E_{Q^\perp}$ have negative real parts. If one of these eigenvalues has algebraic multiplicity not equal to its geometric multiplicity, then there exist solutions with initial conditions in $Q^\perp$ that have the growth $p(t)e^{\lambda t}$, where $p(t)$ is a polynomial of degree at most 2. The exponential decay will win over the polynomial growth in time. Thus, if the linearized Poincaré map turns out to have an eigenvalue that lies outside the open unit disk, we can instead consider the m-th iterate of the Poincaré map and for m large enough it will have all eigenvalues in a closed subset of the open unit disk. We conclude that the stall solution is asymptotically orbitally stable. $\square$

Above we carried out the stability analysis for the first traveling wave solution. We can do the same for the other traveling wave solutions and it turns out that their stability again depends on the eigenvalues of $E|_{Q^\perp}$. Note, however, that we are abusing the notation slightly, because $Q^\perp$ changes from one traveling wave solution to the next, as does E.

Let us now calculate the entries of the 3×3 matrix $E|_{Q^\perp}$ for the j-th traveling wave solution. By the proof of Proposition 3.1 we know that $Q \subset Ker(\overline{\psi_c'})$, so we only need to calculate the action of $\overline{\psi_c'}$ on $Q^\perp$. To this end consider

$$\begin{aligned}
\overline{\psi_c'}(\wp - \bar{\wp}, 0, 0) &= \tfrac{\mu_j}{2\pi} \int_0^{2\pi} (-3b(\wp - e_2) + c)(\wp - \bar{\wp}) d\theta \\
&= \tfrac{\mu_j}{2\pi} \int_0^{2\pi} -\tfrac{b}{2}(\wp^2 - \tfrac{1}{2} g_2) - \tfrac{b}{4} g_2 + 3b\wp\bar{\wp} d\theta
\end{aligned}$$

where we have added and subtracted $\frac{b}{4}g_2$ and integrated out a constant multiple of $\wp - \bar{\wp}$. By using the identity $\wp'' = 6\wp^2 - \frac{1}{2}g_2$ and the fact that $\wp'$ is periodic, we get

$$\begin{aligned}
&= \tfrac{\mu_j}{2\pi} \int_0^{2\pi} -\tfrac{b}{2}\wp'' - \tfrac{b}{4} g_2 + 3b\wp\bar{\wp} d\theta \\
&= \tfrac{b\mu_j}{4}(12\bar{\wp}^2 - g_2).
\end{aligned}$$

Operating on the other two vectors is simpler

$$\begin{aligned}
\overline{\psi_c'}(0, 1, 0) &= \mu_j(3be_2 + c - 3b\bar{\wp}) \\
\overline{\psi_c'}(0, 0, 1) &= 0.
\end{aligned}$$

We now calculate

$$\begin{aligned}
(\nu \tfrac{\partial^2}{\partial \eta^2} + \psi_c')(\wp - \bar{\wp}, 0, 0) &= \tfrac{b\mu_j}{2}(\tfrac{\partial^2}{\partial \eta^2} - 6\wp + 6e_2 + \tfrac{2c}{b\mu_j})(\wp - \bar{\wp}) \\
&= \tfrac{b\mu_j}{2}(\wp'' - 6\wp^2 + 6\wp\bar{\wp}) + \tfrac{b\mu_j}{2}(6e_2 + \tfrac{2c}{b\mu_j})(\wp - \bar{\wp}) \\
&= \tfrac{b\mu_j}{2}(-\tfrac{1}{2}g_2 + 6\wp\bar{\wp} + (6e_2 + \tfrac{2c}{b\mu_j})(\wp - \bar{\wp})).
\end{aligned}$$

This allows us to write down the 3×3 matrix

$$E|_{Q^\perp} = \begin{bmatrix} 3b\mu_j(\bar{\wp} + e_2) + c & -3b\mu_j & 0 \\ \frac{b\mu_j}{4l_c}(12\bar{\wp}^2 - g_2) & \frac{\mu_j}{l_c}(c - 3b(\bar{\wp} - e_2)) & -\frac{1}{l_c} \\ 0 & \frac{1}{4l_c B^2} & -\frac{\gamma}{4l_c B^2}(F_T^{-1})' \end{bmatrix}.$$

Note here that $e_1 \geq e_3 \geq e_2$ are the stationary values of $\wp(\cdot, k_j)$. Because the real period of $\wp$ scales in a simple way with j, one can show that if $e_i(1)$ are the stationary values of $\wp(\cdot, k(\bar{c}_1))$ then $e_i = \frac{e_i(1)}{j}$. Thus, we see that the stationary values e_i and g_2 change in a very simple way with j. Once the constants of integration $\bar{c}_j$ have been determined, the matrix is fully determined and its eigenvalues can be readily calculated.

4 Relaxing the Assumptions $K = I$ and $\gamma = \gamma_*$

Our goal in this section is to prove that when $E_{Q^\perp}$ has no eigenvalues on the imaginary axis, then for K close to the identity and γ close to γ_*, there exists a unique stall solution close to the special one already constructed which has the same stability properties. This follows from the Implicit Function Theorem. Recall that by making $am = 0$ we set $K = I$.

Theorem 4.1 *Let $\bar{x}$ be a stall solution given by Proposition 2.1 and assume that the eigenvalues of $E_{Q^\perp}$ lie off the imaginary axis. There exists a neighborhood V of $(\gamma_*, 0) \in \mathbf{R}^2$ and a neighborhood U of $\bar{x} \in X$ such that for any $(\gamma, am) \in V$ there exists a unique periodic solution $x \in U$. Furthermore, x is asymptotically stable (unstable) if $\bar{x}$ is asymptotically stable (unstable).*

Proof: We already showed in [6] that the solutions of (1 -3) depend smoothly on the parameters γ and am. We conclude that the Poincaré map will also depend smoothly on these parameters.

Our strategy is now to apply the Inverse Function Theorem to the Poincaré map, P, associated with $\bar{x}$. $\bar{x}$ is a fixed point for P and P linearized about this solution, $DP(\bar{x})$, has a spectrum that is bounded away from the unit circle. In particular it is bounded away from 1 and thus $DP(\bar{x}) - I$ is invertible with a bounded inverse. It now follows from the Implicit Function Theorem that there exists a continuous two parameter family of fixed points of P, $\{x\}_{(\gamma,am)\in V}$. For each $(\gamma, am) \in V$ the fixed point x is a periodic solution of (1-3).

If $E_Q^\perp$ has eigenvalues with negative real parts then $DP(\bar{x})$, or the linearization of some iterate of P, will be a contraction, i.e. there exists a constant $0 \leq \beta < 1$ such that $\|DP(\bar{x})y_0\| \leq \beta\|y_0\|$ for all y_0. Since P depends smoothly on (γ, am), so does DP. In particular, by taking V small enough we can guarantee that $\|DP(\bar{x}) - DP(x)\| \leq \frac{1-\beta}{2}$. We can now conclude that

$$\|DP(x)y_0\| \leq \beta\|y_0\| + \frac{1-\beta}{2}\|y_0\| < \frac{1+\beta}{2}\|y_0\|,$$

i.e. $DP(x)$ is also a contraction. It follows that the orbit x is asymptotically orbitally stable.

Assume now that $E_Q^\perp$ has an eigenvalue λ with a positive real part. The eigenvalue of $DP(\bar{x})$ corresponding to λ will be an isolated eigenvalue outside the unit disk. Since $DP(x)$ is a relatively bounded perturbation of $DP(\bar{x})$, any isolated eigenvalue will depend continuously on (γ, am) (see Kato [14]). Hence, by making V small enough we guarantee that $DP(x)$ has an eigenvalue outside the unit disk and x is an unstable orbit. $\square$

5 Numerical Simulations

In this section we present numerical simulations of stall in four different cases: Figure 5.1 shows $\gamma = \gamma_*, K = I$, Figure 5.2 shows $\gamma = \gamma_*$ and a general K, Figure 5.3 shows a general γ and $K = I$ and finally Figure 5.4 shows both general γ and K. These four different cases give a good indication of how the the two parameters γ and am affect the shape of the traveling wave solution. Increasing γ tends to make the trough be deeper and narrower, whereas decreasing it will do the opposite. We only display what happens for $\gamma \geq \gamma_*$. Increasing am tends to skew the shape of the traveling wave. The case for $am < 0$ is not of physical interest so we omit it here. For completness we also present a numerical simulation of surge in Figure 5.5. As the numerics show, surge is a periodic orbit in the two variables (Φ, Ψ) where $\varphi = 0$.

These numerical solutions are calculated using a Lax-Wendroff finite difference scheme. The spatial resolution for the variable φ is 128 points. The initial conditions are set so that φ has the shape of a sinus wave with small amplitude to seed the instability and the variables Φ and Ψ are set slightly off their equilibrium position for the case when $\varphi = 0$. We let the simulation run for a long time and then take a snapshot of the stall cell when it has stabilized.

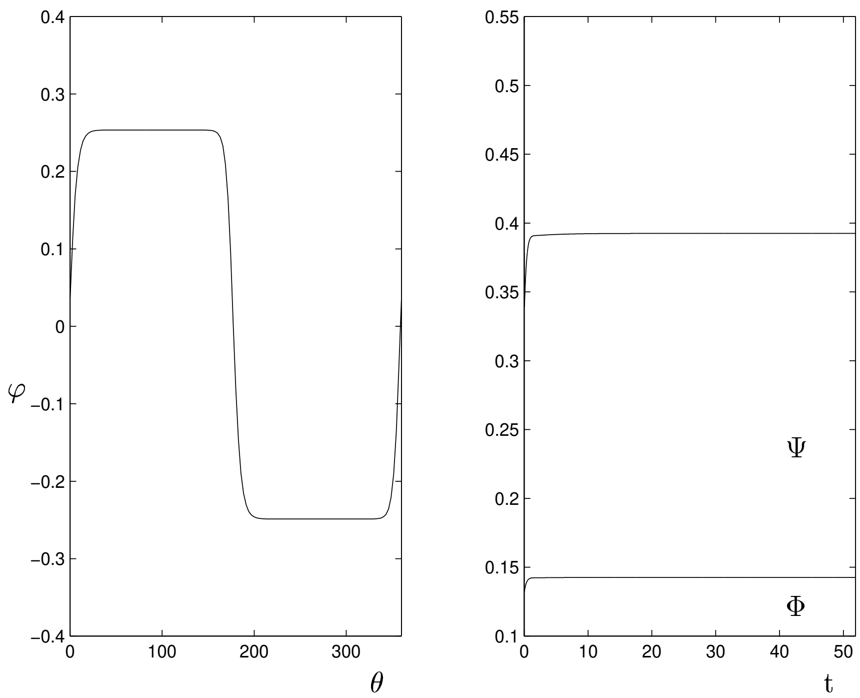

Figure 5.1: This figure shows the shape of a stall cell in the special case when $\gamma = \gamma_*$ and $K = I$. The left hand plot shows a snap shot of the stall cell after the transient has died out. The right hand plot shows how the two variables (Φ, Ψ) approach constant values quickly.

Note that by choosing the modulus correctly in the Jacobi ns function, one can make it fit the above stall shape well.

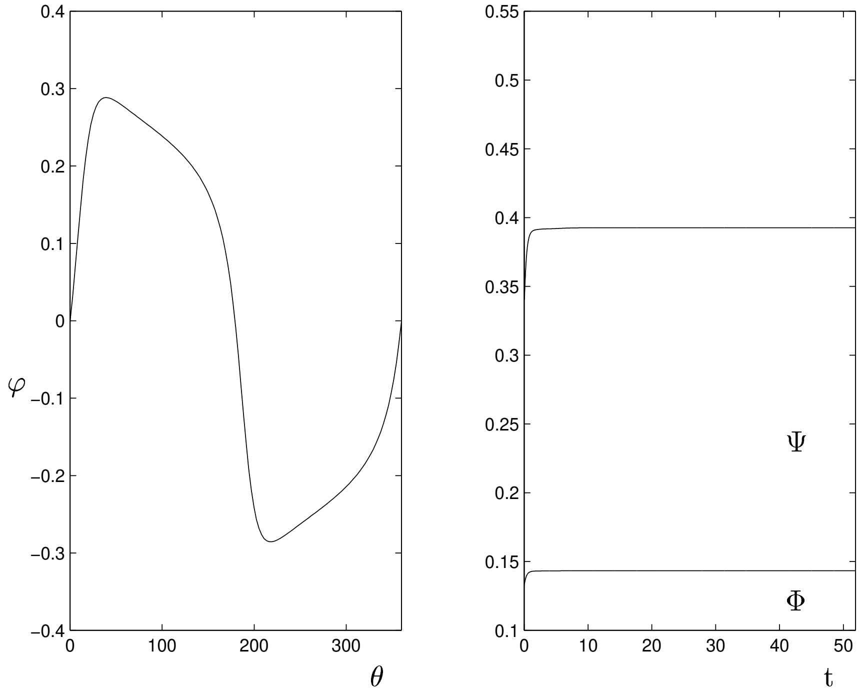

Figure 5.2: This figure shows the shape of a stall cell in the special case when $\gamma = \gamma_*$ and K is not the identity. This skews the shape of the stall cell, but the trough and the peak are still identical in shape.

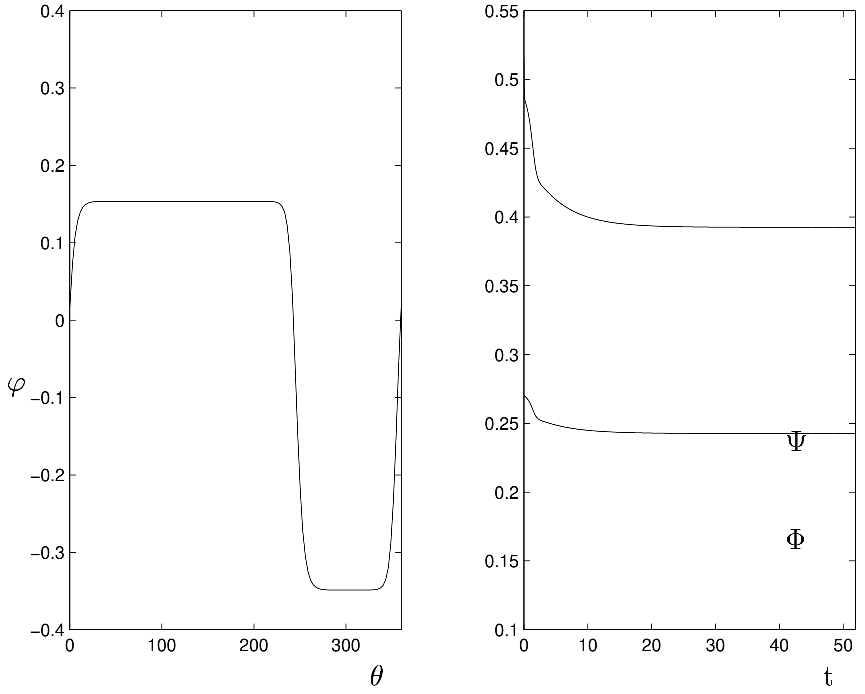

Figure 5.3: This figure shows the shape of a stall cell in the special case when γ is not equal to γ_* but $K = I$. This shows how the shape of the trough is no longer the same as the shape of the peak, i.e. the trough becomes narrower and deeper while the peak becomes wider and lower.

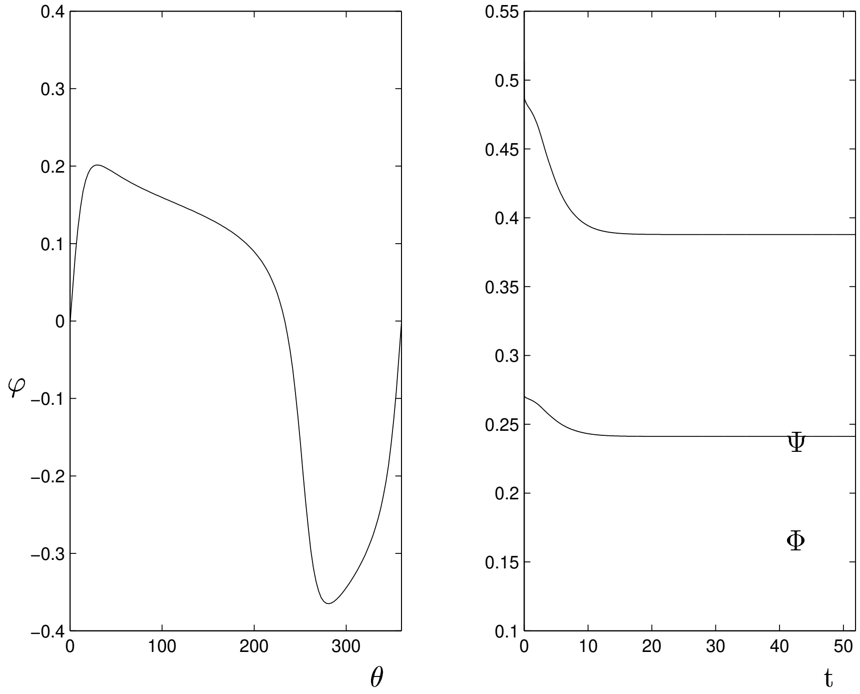

Figure 5.4: This figure shows the shape of a stall cell in the general case when γ is arbitrary and K is not the identity. Here we see that the shape of the stall cell is skewed and the width and depth/height of the trough/peak has changed in the same way it did in Figure 5.3.

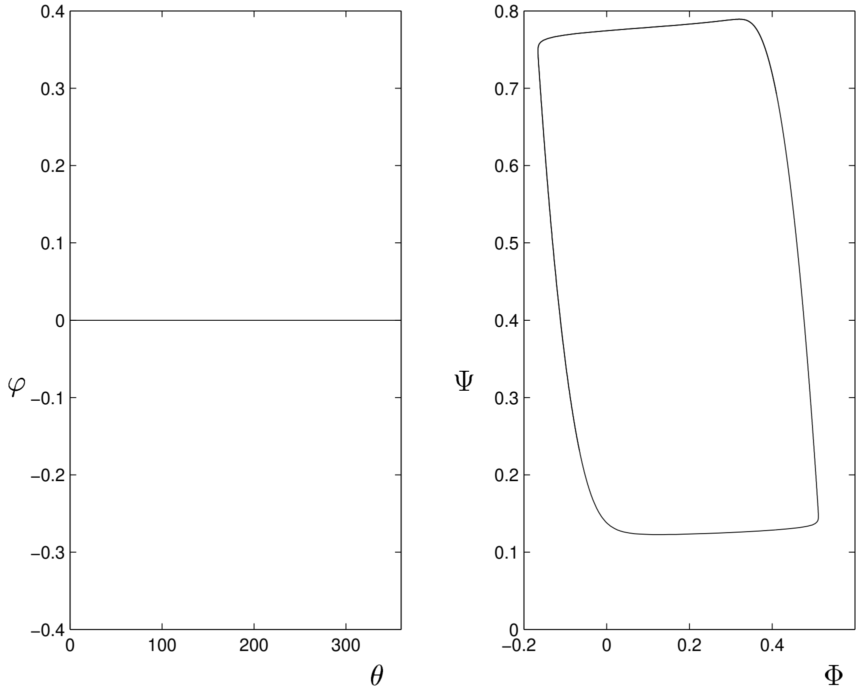

Figure 5.5: This figure shows the surge cycle after the transient has died out. Here we clearly see that surge is a periodic orbit in the (Φ, Ψ) plane and $\varphi = 0$.

In general the speed of the traveling wave is going to depend on the parameters am and γ. We calculated this speed numerically and Figure 5.6 shows the results of these runs. It indicates that the value of γ has little effect on the propagation velocity, whereas the value of am has a considerable effect on the velocity. The velocity here is measured in revolutions per time unit.

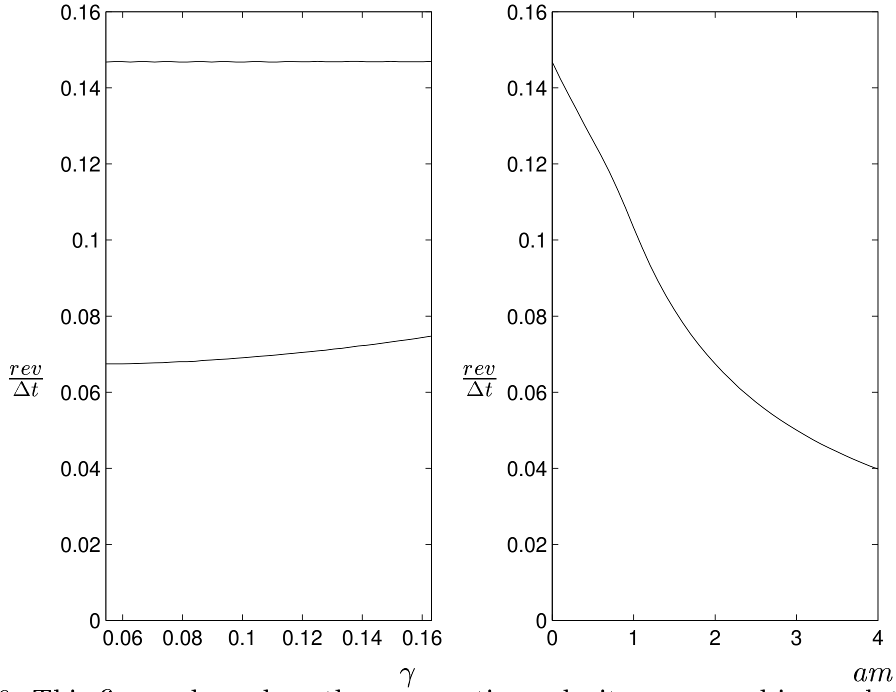

Figure 5.6: This figure shows how the propagation velocity, measured in revolutions per time unit, of the rotating stall cell changes with γ and am. On the left hand side we have plotted the propagation velocity as a function of γ first for $am = 0$, i.e. $K = I$, (the higher curve) and then for $am = 2.0$ (the lower curve). This plot indicates that the velocity does not depend strongly on γ for γ close to γ_*. On the right hand side we plotted the propagation velocity as a function of am for $\gamma = \gamma_*$. This shows that the velocity changes considerably with am.

A curious observation is that the value of am also affects the growth rate of the initial disturbance, as it grows into a stall cell. Larger am has a damping effect on the growth.

Finally we show here a plot of the largest real part of the eigenvalues of the matrix $E|_{Q^\perp}$ as a function of the parameter B, which represents the size of the plenum (see Figure 5.7). Here we have chosen the eddy viscosity constant to be $\nu = 0.15$. According to the inequality (5) there only exist three stall cells in this case. Figure 5.7 shows that they are all stable for a large range of B, but are, however, only marginally stable as B becomes large. This is consistent with frequently reported findings that compressors with small B values typically stall whereas compressors with large B values typically surge.

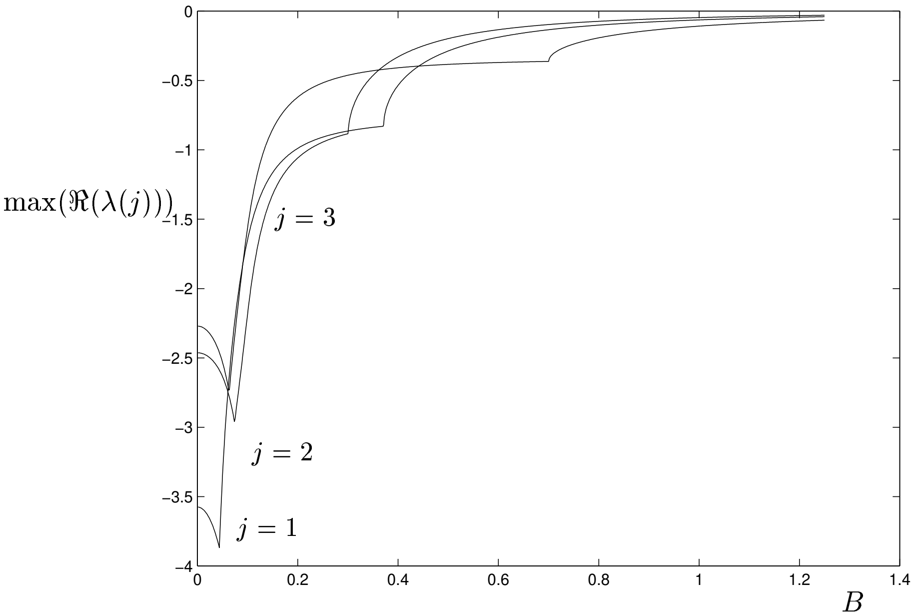

Figure 5.7: Here we see the largest real part of the eigenvalues of the matrix $E|_{Q^\perp}$ plotted for the four stall cell solutions, $j = 1, 2, 3$. Note that the stall solutions are all stable, but are only

marginally stable for large B values.

We can now conclude that for the parameter values chosen here, for γ close to γ_* and for small B the basic attractor contains three stall solutions. For B large it contains three or fewer stall solutions. In general, the basic attractor will contain none to several stall solutions for γ close to γ_* and for small B, but for larger B values it will contain as many or fewer stall cells. This of course does not exclude the possibility that it also contains surge or even classic surge.

6 Conclusion

It is known that for large γ, the only stable solution of the viscous Moore-Greitzer equation is the axisymmetric design flow [19]. Therefore, for large γ, the basic attractor, $\mathcal{B}$, conists only of the stationary solution that represents design flow. As γ is decreased, the stationary solution undergoes a sequence of subcritical Hopf bifurcations. These bifurcations will each create surge or a stall solution. The stall solutions are created in order, lower to higher number of nodes [1] [19].

When one considers the Poincaré map of the flow, then generically stall and surge will appear as saddle node bifurcations away from the design flow, see Figure 5.8. The stable branch represents a periodic orbit which belongs to the basic attractor $\mathcal{B}$, whereas the unstable branch lies in the remainder $\mathcal{C}$. The unstable branch connects to the point where the design flow undergoes subcritical Hopf bifurcation. Figure 5.8 shows the bifurcation diagram for either surge or a stall solution.

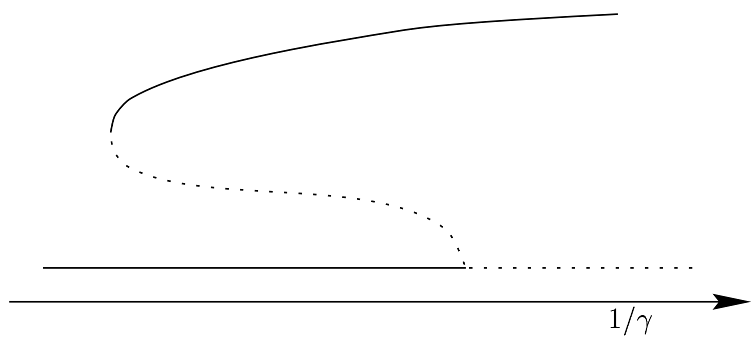

Figure 5.8: This figure shows how the Poincaré map of the flow undergoes saddle node bifurcation. Each branch created at the saddle node represents a periodic orbit in the original flow. The straight line represents design flow which becomes unstable for small enough γ.

When γ has been decreased all the way down to γ_* we will have created a few stable stall solutions which are only marginally stable when B is large. The design flow solution is unstable and surge only exists and is stable for large B values [19].

We can conclude that for $\gamma = \gamma_*$ and B small the basic attractor contains a few stall solutions and no design flow or surge component. When B is large it consists of as many or fewer stall solutions and a surge component. When γ increases, design flow will become stable and hence be a component of the basic attractor, and when γ becomes large enough it will be the only component in the basic attractor. The existence and the relevant parameter range of a classic surge component has not been addressed here, we will do so in a separete paper.

7 Acknowledgements

We would like to thank Igor Mezić for valuable input on modeling issues. Furthermore we would like to thank Andrzej Banaszuk, Petar Kokotović, Christopher K. R. T. Jones and Brianno Coller for fruitful discussions. We would also like to gratefully acknowledge funding by Nýsköpunarsjódur Námsmanna, NSF grants DMS-9704874, DMS-9628606 and PHY-9601954, LACOR grant number 4157U0015-3A from Los Alamos National Laboratory and a travel grant from AFSOR under grant number F49620-95-1-0409.

References

[1] R.A. Adomaitis and E.H. Abed. Local nonlinear control of stall inception in axial flow compressors. *29th Joint Propulsion Conference and Exhibit*, 1993. AIAA Paper 93–2230.

[2] A. Banaszuk, H.A. Hauksson, and I. Mezić. A backstepping controller for a nonlinear partial differential equation model of compression system instabilities. *SIAM J. of Control and Optimization, submitted*, 1998.

[3] B.Birnir and R.Grauer. The global attractor of the damped and driven sine-Gordon equation. *Comm. Math. Phys.*, 162:539–590, 1994.

[4] B. Birnir. An example of blow-up for the complex KdV equation and existence beyond the blow-up. *SIAM J. of Appl. Math.*, 47(4):710–725, 1987.

[5] B. Birnir. Global attractors and basic turbulence. In K.M. Spatschek and F.G.Mertens, editors, *Nonlinear Coherent Structures in Physics and Biology*, volume 329, New York, 1994. NATO ASI Series.

[6] B. Birnir and H.A. Hauksson. Finite dimensional attractor of the Moore-Greitzer PDE model. *SIAM J. of Applied Math.*, 59(2):636–650, 1998.

[7] I.J. Day. Axial compressor performance during surge. *Journal of Propulsion and Power*, 10(3):329–336, 1994.

[8] J.F. Escuret and V. Garnier. Numerical simulations of aerodynamic flow instabilities in axial compressors. *Von Karman Institute for Fluid Dynamics: 1995-1996 Lecture Series*, 1996.

[9] E.M. Greitzer. Surge and rotating stall in axial flow compressors, Part II. *Trans. ASME, Journal of Engineering for Power*, pages 199–217, 1976.

[10] C. Hermite. *Oeuvres de Charles Hermite*, volume 3. Paris: Gauthier-Villar, 1912.

[11] B.R. Hunt, T. Sauer, and J.A. Yorke. Prevalence: A translation-invariant "almost every" on ininite-dimensional spaces. *Bull. of the Am. Math. Soc.*, 27(2):217–238, 1992.

[12] E.L. Ince. *Ordinary Differential Equations.* Dover, 1956.

[13] J.Guckenheimer and P.Holmes. *Nonlinear Oscillations, Dynamical Systems, and Bifurcations of Vector Fields.* Springer, 1983.

[14] T. Kato. *Perturbation Theory for Linear Operators.* Springer, 1980.

[15] D.F. Lawden. *Elliptic Functions and Applications.* Springer, 1989.

[16] W. Magnus and W. Wrinkler. *Hill's Equation.* Willey-Interscience, 1966.

[17] C. A. Mansoux, D. L. Gysling, J. D. Setiawan, and J. D. Paduano. Distributed nonlinear modeling and stability analysis of axial compressor stall and surge. In *Proc. American Control Conference*, pages 2305–2316, 1994.

[18] F.E. McCaughan. Numerical results for axial flow compressor instability. *ASME Journal of Turbomachinery*, 111:434–441, 1989.

[19] F.E. McCaughan. Bifurcation analysis of axial flow compressor stability. *SIAM Journal of Applied Mathematics*, 50:1232–1253, 1990.

[20] I. Mezić. A large-scale theory of axial compression system dynamics. *preprint*, 1998.

[21] J. Milnor. On the concept of attractor. *Communications in Mathematical Physics*, 99:177–195, 1985.

[22] F.K. Moore and E.M. Greitzer. A theory of post-stall transients in axial compression systems:Part 1 - Development of equations. *ASME Journal of Engineering for Gas Turbines and Power*, 108:68–76, 1986.

[23] P. Du Val. *Elliptic Functions and Elliptic Curves.* Cambridge University Press, 1973.

[24] A.G. Wilson and C. Freeman. Stall inception and development inan axial flow aeroengine. *Trans. ASME, Journal of Turbomachinery*, 116:216–225, 1994.